

AD-A046 908

WASHINGTON UNIV SEATTLE APPLIED PHYSICS LAB
COMPUTER SIMULATION OF FULL-SIZE, HIGH-DRAIN AGCL-MG WATER-ACTI--ETC(U)
SEP 71 D W FALETTI
APL-UW-7112

F/G 10/3

N00017-71-C-1305

NL

UNCLASSIFIED

| of |
ADA046908



END
DATE
FILMED
12-77
DDC

AD A U 46908



APPLIED • PHYSICS • LABORATORY
A DIVISION OF THE UNIVERSITY OF WASHINGTON

DISTRIBUTION STATEMENT A

Approved for public release;
Distribution Unlimited

①

⑥

**Computer Simulation of Full-Size, High-Drain
AgCl-Mg Water-Activated Batteries
with AZ61 and AP65 Anodes,**

⑩

by ^{Dwane} D.W. Faletti

⑫ 31 p.

⑭

APL-UW-7112

⑪

15 September 1971

⑮

WAPP 17-71-C-1345

ACCESSION for	
NTIS	White Section <input checked="" type="checkbox"/>
DDC	Buff Section <input type="checkbox"/>
UNANNOUNCED	<input type="checkbox"/>
JUSTIFICATION	
Per Hqs. on file	
BY _____	
DISTRIBUTION/AVAILABILITY CODE	
Dist.	AVAIL. and/or SPECIAL
A	

1477
031 700

DISTRIBUTION STATEMENT A
Approved for public release;
Distribution Unlimited

of

DDC
RECEIVED
NOV 15 1977

D 4B

CONTENTS

INTRODUCTION..... 1

CHARACTERISTICS OF THE MK 61 (MOD 0 AND MOD 2), MK 64, AND
MK 67 BATTERIES..... 1

RESULTS..... 3

 The Mk 61 Mod 0 Battery..... 7

 The Mk 61 Mod 2 Battery..... 7

 The Mk 64 Battery..... 8

 The Mk 67 Battery..... 8

DISCUSSION..... 10

APPLICATIONS..... 11

ACKNOWLEDGMENT..... 11

REFERENCES..... 12

ABSTRACT

The predictions of a computer simulation for high-drain, AgCl-Mg batteries are compared to the observed performance of four full-size AgCl-Mg batteries: the Mk 61 (Mod 0 and Mod 2), Mk 64 and Mk 67. The Mk 61 Mod 0, like the Mk 64 and Mk 67 batteries, uses AZ61 magnesium anodes; the Mk 61 Mod 2 uses the high voltage magnesium alloy, AP65. These four batteries differ sufficiently in their configurations and were discharged over a wide enough range of operating conditions to constitute a valid test of the computer simulation's capabilities. The simulation gave voltage predictions accurate to within 7% for over 90% of the discharge. Predictions for other useful parameters, such as electrolyte temperature, are also given. This simulation can eliminate the need for most of the "cut and try" effort presently required in AgCl-Mg battery development and should be helpful in system studies of this battery.

INTRODUCTION

Present design techniques for high-drain, water-activated, AgCl-Mg batteries require considerable experimentation involving the construction and testing of subassemblies as well as full-size prototypes. The operating conditions for such batteries often encompass a wide range of temperature, salinity, and pressure conditions. Limited discharge facilities and the expense of in-water tests make it unfeasible to test water-activated batteries over their entire operating envelope, thus increasing the technological development risk.

A computer simulation, which was developed as an aid to the design of AgCl-Mg water-activated batteries, has been described (References 1 and 2). Here we will compare the agreement between that simulation's predictions and the observed behavior of four full-size, high-drain batteries. Of these batteries, the Mk 61 Mod 0, Mk 64, and Mk 67 all use AZ61 magnesium alloy for their anodes. The Mk 61 Mod 2 uses the high voltage alloy AP65¹ for its anodes. The batteries differ sufficiently in their configurations and were discharged over a wide enough range of operating conditions to constitute a valid test of the capabilities of the simulation.

CHARACTERISTICS OF THE MK 61 (MOD 0 AND MOD 2), MK 64, AND MK 67 BATTERIES

The Mk 61 Mod 0 and Mod 2, Mk 64 and Mk 67 are high-drain, water-activated batteries which use a compact, rugged, lightweight, pile-type construction (Fig. 1). Glass beads embedded in the cathodes act as separators, permitting electrolyte to pass between the electrodes of the cell. Metal separators are placed between adjacent cells to prevent unwanted electrochemical reactions and to provide electrical contact.

In the pile-type construction parasitic currents flow between cells of different potential because the cells are immersed in a continuous electrolyte. The parasitic currents act as a load in parallel to the external load, causing lower battery voltage and a reduced discharge life. The magnitude of the parasitic currents increases with the conductivity and volume fraction of the electrolyte, the area of the flow passages above and below the battery, and the cross-sectional area of the flow passages within the cells.

Of the four batteries, the Mk 64 operates at the highest current density and has a parasitic-to-external current ratio of less than 0.05. The Mk 61 battery, which has the same flow passage area and cell configuration but operates at about half the current density, has a ratio near 0.08. The Mk 67 battery operates with a voltage control system which has the effect of increasing the conductivity of the electrolyte as the discharge progresses; thus, its parasitic-to-external current ratio increases during the discharge and, depending upon the

¹AP65 is also called GEMAG or MELMAG.

temperature and composition of the entering electrolyte, ranges from 0.19 to 0.25 in the early portions of the discharge, 0.25 to 0.33 when the discharge is 90% complete, and 0.67 to 0.85 at the completion of the discharge.

The cells of the battery may be connected in series as in Fig. 1, or they may be divided into two series-connected sections which are connected in parallel to the load as in Fig. 2. The Mk 64 battery has 161 cells connected electrically in series; the Mk 61 Mod 0, Mk 61 Mod 2, and Mk 67 batteries all have two sections connected electrically in parallel, each section containing 118, 104, and 230 cells, respectively.

The Mk 61 and Mk 64 batteries have cells and flow passages of the same size and shape (Table I and Fig. 3) and are designed to operate at near the same power level. Since the Mk 64 has a single section and the Mk 61 has two, the current density is nearly twice as high and the discharge period is correspondingly shorter for the former.

The cells of the Mk 67 battery are rectangular in shape and are about two and one-half times larger than the Mk 61 and Mk 64 cells (Table I and Fig. 3). The Mk 67 cathodes have about one-third greater capacity per unit area than those of the Mk 61 and Mk 64 batteries.

The Mk 61 and Mk 64 batteries operate with an entering electrolyte of constant flow rate. This produces battery voltages which are strongly dependent on electrolyte composition and temperature, and which fall continuously as the discharge progresses.

The Mk 67 battery is designed to operate within a few percent of 245 V over the range of sea water temperature and composition found in the world's oceans. This is accomplished by a voltage control system that recirculates a constant flow rate of effluent back into the lower flow passage and adjusts the flow rate of entering sea water to achieve the desired voltage (Fig. 4).

Table I. Summary of Battery Configurations

	Mk 61 Mod 0	Mk 61 Mod 2	Mk 64	Mk 67
No. of cells	236	208	161	460
No. of parallel-connected sections	2	2	1	2
Cathode area, cm ²	396	393	396	1097
Cathode thickness, cm	0.038	0.037	0.038	0.055
Anode thickness, cm	0.028	0.028	0.028	0.033
Electrode separation, cm	0.058	0.058	0.058	0.058
Area of flow passage, cm ²	10.24	10.24	10.24	67.25

These particular batteries were chosen for this study because (a) their physical dimensions and method of manufacture and testing were well documented, and (b) the four batteries differed sufficiently in operating conditions and physical configurations to provide a good test of the computer simulation's capabilities.

RESULTS

The computer simulation's predictions are compared to observed battery voltages, effluent electrolyte temperatures, and (for the case of the Mk 67 battery) electrolyte flow rates in Figs. 5-29. The observed values lie within the crosshatched areas on the figures² and were obtained from discharges conducted by the Quality Evaluation Laboratory of the Naval Torpedo Station, Keyport, Washington.

The manufacturing tolerances, and to a lesser extent the test tolerances of these batteries, allow a significant spread in battery performance. A measure of the maximum possible spread in performance was obtained by making three computer simulations for each test condition studied. These were (a) for the case where the battery was built according to the nominal specified dimensions and tested according to the nominal specified test conditions, (b) for the case where the battery was built with the most favorable set of dimensions allowed by the specifications and tested according to the most favorable set of operating conditions permitted by the test specifications, and (c) for the case of the least favorable set of dimensions permitted and the least favorable set of operating conditions permitted. These three conditions are referred to as the nominal, best, and poorest performance predictions, respectively, and are represented by the solid lines in Figs. 5-29.

The computer inputs for battery dimensions and discharge conditions are given in Tables II, III, IV and V. Two other computer inputs warrant discussion. The computer simulation makes use of numerical analysis to account for spatial and temporal variations within these batteries. This is done by dividing the cells into a sufficiently large number of subcells so that spatial variations in operating conditions within any subcell are small, and by dividing the discharge period into short time intervals so that temporal variations within a time interval are small. For this study we chose 25 subcells and a 10-sec time interval. This was shown to be adequate by making checks in which the number of subcells was increased to 100 and the time intervals decreased to 1 second. Only negligibly small changes in the computer predictions were observed.

²Except for the Mk 61 Mod 2 discharges where the number of discharges was small enough to permit plotting individual discharges.

Table II. Battery Dimensions for the Mark 61 Mod 0 and Mark 64 Battery Simulations

	Performance		
	<u>Poor</u>	<u>Nominal</u>	<u>High</u>
Cathode area, cm ²	394.29	395.72	397.14
Cathode thickness, cm	0.0356	0.0381	0.0406
Anode thickness, cm	0.0254	0.0279	0.0305
Silver foil thickness, cm	0.0013	0.0019	0.0025
Electrode separation, cm	0.0686	0.0584	0.0483
Cell thickness, cm	0.1309	0.1264	0.1219
Width of bottom and top opening of cells, cm	10.002	10.002	10.002
Width of tape at top and bottom of cells, cm	0.2654	0.3112	0.3569
Thickness of tape at top and bottom of cells, cm	0.0025	0.0025	0.0025
Area of flow passage above (or below) the battery, cm ²	10.38	10.24	10.09

Table III. Battery Dimensions for the Mark 61 Mod 2 Battery Simulation

	Performance		
	<u>Poor</u>	<u>Nominal</u>	<u>High</u>
Cathode area, cm ²	391.0	392.5	394.0
Cathode thickness, cm	0.0356	0.0368	0.0381
Anode thickness, cm	0.0254	0.0279	0.0305
Silver foil thickness, cm	0.0016	0.0019	0.0022
Electrode separation, cm	0.0660	0.0584	0.0508
Cell thickness, cm	0.1286	0.1251	0.1215
Width of bottom and top opening of cells, cm	10.57	10.47	10.37
Width of tape at top and bottom of cells, cm	0.4191	0.4826	0.5461
Thickness of tape at top and bottom of cells, cm	0.0025	0.0025	0.0025
Area of flow passage above (or below) the battery, cm ²	10.46	10.24	10.02

Table IV. Test Conditions for the Mark 61 and Mark 64 Battery Simulations

	Mk 61 Mod 0, R=0.58 ohm			Mk 61 Mod 0, R=0.72 ohm			Mk 61 Mod 2			Mk 64		
	Performance	High	Low	Performance	High	Low	Performance	High	Low	Performance	High	Low
Load Resistance, ohm	0.578	0.580	0.582	0.718	0.720	0.722	0.718	0.720	0.722	0.673	0.675	0.677
Pressure, atm	3.992	4.065	4.130	1.952	2.011	2.088	1.952	2.020	2.088	2.088	2.156	2.225
Electrolyte												
Flow Rate, gal/min	10.2	10.0	9.8	9.8	9.6	9.4	9.8	9.6	9.4	10.2	10.0	9.8
Temperature, °C												
High temp.	30.00	31.11	32.22	30.00	31.11	32.22	30.00	31.11	32.22	30.0	31.0	32.0
Ambient temp.	14.44	15.55	16.66	11.97	12.80	13.63	11.97	12.80	13.63	11.97	12.8	13.63
Low temp.	0.00	0.833	1.666	0.0	0.833	1.666	0.0	0.833	1.666	0.0	0.833	1.666
Salinity, ‰												
High temp.	37.0	38.0	39.0	30.0	31.0	32.0	30.0	31.0	32.0	30.0	31.0	32.0
Ambient temp.	30.0	31.0	32.0	30.0	31.0	32.0	30.0	31.0	32.0	30.0	31.0	32.0
Low temp.	30.0	31.0	32.0	30.0	31.0	32.0	30.0	31.0	32.0	30.0	31.0	32.0

*Table V. Battery Dimensions and Test Conditions
for the Mark 67 Battery Simulation*

	Performance		
	<u>Low</u>	<u>Nominal</u>	<u>High</u>
Battery Dimensions			
Number of cells	460	460	460
Number of sections	2	2	2
Cathode area, cm ²	1086.13	1097.48	1108.77
Cathode thickness, cm	0.05207	0.05461	0.05715
Anode thickness, cm	0.03048	0.03302	0.03556
Silver foil thickness, cm	0.00127	0.00190	0.00254
Electrode separation, cm	0.06604	0.05842	0.05334
Cell thickness, cm	0.1397	0.1480	0.1562
Width of bottom and top opening of cells, cm	22.9387	22.8473	22.7558
Width of tape at top and bottom of cells, cm	0.1359	0.2649	0.3937
Thickness of tape at top and bottom of cells, cm	0.0025	0.0025	0.0025
Area of flow passage above (or below) the battery, cm ²	67.84	67.25	66.67
Test Tolerances			
Load resistance, ohm	0.435	0.438	0.441
Pressure, atm	3.72	4.06	4.40
New electrolyte flow rate, gal/min			
Maximum	122.0	120.0	118.0
Minimum	17.0	15.0	13.0
Recirculation flow rate, gal/min	32.0	36.0	40.0
Electrolyte temperature, °C			
High temp.	29.4	30.8	32.2
Ambient temp.	10.0	12.8	15.6
Low temp.	0.0	0.0	0.56
Electrolyte salinity, ‰			
High temp.	35.0	37.5	40.0
Ambient temp.	30.0	35.0	40.0
Low temp.	7.5	10.0	12.5

The Mk 61 Mod 0 Battery

Figures 5-8 present a comparison between the predicted and observed voltages for the Mk 61 Mod 0 battery.³ These four test conditions encompass four levels of temperature (0.8, 12.8, 15.6 and 31.1°C) as well as two levels of salinity (31 and 38‰), pressure (15 and 45 psig), and resistance (0.72 and 0.58Ω).

The computer simulation predicts low voltages in the early part of the discharge, and therefore the predicted discharge periods are too long. A significant number of the batteries performed better than the highest predictions of the computer simulations in all four test conditions. Thus, unless the batteries were built or tested outside of the allowed tolerances, it must be concluded that the voltage predictions for the Mk 61 battery are intrinsically low. However, the magnitude of this discrepancy is not large, especially in view of the 6% spread in observed voltages and the 5-20% spread in the observed discharge time to a cutoff voltage of 100 V (0.85 V/cell). By comparison, with the same cutoff voltage the predicted voltages are within 6% of the observed voltages (taken to be the center line of the observed voltage envelope) for 100% of the low temperature discharges (Fig. 5), 92% for the two sets of discharges near 15°C (Figs. 6, 7), and 97% for the high temperature discharges (Fig. 8).

The predicted and observed Mk 61 Mod 0 effluent temperatures are compared in Figs. 9-12. Except for starting transients caused mainly by the limitations of the test facility, the observed and predicted temperatures are in good agreement. The predicted temperatures would have to be about 1 to 2°C higher to be consistent with the voltage predictions. However, this is not much larger than the uncertainties in temperature measurement and is well within the accuracy required for battery design.

The Mk 61 Mod 2 Battery

The Mk 61 Mod 2 battery differs from the Mk 61 Mod 0 battery primarily in that its anodes are made of AP65 magnesium alloy. This permits a reduction in the number of cells from 236 in the Mk 61 Mod 0 to 208 in the Mod 2 battery.

The predictions of the computer simulation are compared to the observed voltages in Figs. 13-15. The predicted voltages for the case of a battery built to nominal dimensions and tested according to the nominal values for the discharged specifications are from 3% to 7% lower than the observed voltages during the first three-fourths of the discharge. Thereafter, the observed voltages fall below the predicted voltages. The predicted voltages are high in the latter portions of the discharge because the lower predicted discharge rate causes a longer predicted discharge life.

³This battery uses AZ61 anodes.

The agreements between the observed and predicted voltages obtained for the Mk 61 Mod 2 battery are similar to those obtained with the Mk 61 Mod 0 battery. Since the difference between the Mod 2 and the Mod 0 is that the former uses AP65 anodes instead of AZ61 anodes, these results indicate that the voltage predictions of the computer simulation are equally good for both alloys.

The predicted and observed Mk 61 Mod 2 effluent temperatures are compared in Figs. 16-18. As is the case with the Mk 61 Mod 0 the observed and predicted temperatures are in good agreement with the computer simulation predicting temperatures 1° to 3°C higher than that which would be consistent with the voltage predictions.

The Mk 64 Battery

The Mk 64 battery is designed to operate at the same power level as the Mk 61 but for a shorter period of time. Since it has only one section compared to the Mk 61's two, and since the cells are the same size (Table I), the current density is roughly twice as high.

The observed voltages (taken to be the center line of the observed voltage envelope) are within 2% of the nominal predicted voltage until the observed voltage drops to 100 V (0.62 V/cell) at 3.7 min (Fig. 19). The accuracy of the simulation decreases between 3.7 and 5.2 min with a maximum error of +15% occurring at 4.5 min. The low predictions of the simulation beyond 5.4 min are the result of the higher predicted exhaustion rate during the 3.7 to 5.2 min period.

The errors at or below 100 V result from the limitations of the semi-empirical model upon which the simulation is based (Refs. 1 and 2). Fortunately, enough is known about these limitations that the operating regions where serious errors might be expected can be identified. In practice, this is not a serious consideration since the model works well over the range of operating conditions of interest in modern battery design.

Observed and predicted effluent temperatures are in excellent agreement (Fig. 20). The computer simulation's slightly high temperature predictions are consistent with the slightly high voltage predictions.

The Mk 67 Battery

The Mk 67 battery was tested for three conditions: (a) high temperature, high salinity (Figs. 21-23), (b) ambient temperature, normal salinity (Figs. 24-26), and (c) low temperature, low salinity (Figs. 27-29). The high temperature, high salinity discharges will be discussed first.

Although the Mk 67 battery is designed to operate at 245 V, the performance of the battery is such that even at its maximum flow rate of 120 gal/min the voltage does not fall to 245 V until the 7 to 9 minute mark for the high temperature, high salinity discharge conditions (Fig. 21). This permitted us to determine the adequacy of the computer simulation for the Mk 67 battery when discharged at constant flow rate. The agreement is excellent, with the simulation predicting voltages accurate to better than 1% for the first 5 min and to within 2% until the 8-min mark.

At the 8-min mark the observed voltages begin to fall approximately 0.8 min earlier than that predicted by the "low performance" predictions of the simulation. An examination of the flow rate data for this condition (Fig. 23) shows that the experimental reductions in flow rate lag behind those of the simulation. This lag in flow reduction, which is caused by equipment limitations, explains much of the discrepancy found after 8 min. Another possible source of low observed voltage, especially at low flow rates, is that significant amounts of H_2 are quite likely recirculated into the lower flow passage by the recirculation pump (Ref. 3). This is most likely to occur near the end of the discharge when flow rates are low, because of the increasing volume fraction of H_2 at low flow rates. In spite of this, the predicted and observed discharge life agreed to 5%, based upon the "nominal" computer predictions and the average observed time to 160 V (0.7 V/cell).

The predicted and observed temperatures are in excellent agreement for the first 4 min of the discharge where the flow is constant at 120 gal/min (Fig. 22). Thereafter, the observed temperatures were lower than the predicted temperatures, reflecting the high observed flow rates (Fig. 23) that were responsible for the low observed voltages described above.

The comparisons between the predicted and observed voltages, temperatures, and flow rates when the Mk 67 battery is discharged at 12.8°C are presented in Figs. 24, 25 and 26, respectively. The nominal voltage predictions are within a few percent of the observed voltages for 96% of the discharge period to a cutoff voltage of 160 V (0.7 V/cell).

The temperature and flow predictions are in good agreement with the observed results over most of the discharge (Figs. 25 and 26). During this period, which ends at about 7½ to 8 min, the computer predictions imply that the Mk 67 battery is performing between the nominal and the best expected of it. Thereafter, the observed flow rates decrease and the observed temperatures

"The "best", "nominal" and "poorest" lines on Fig. 22 illustrate the relationship between the "intrinsic" performance of a Mk 67 battery and its effluent temperature. During the period when the flow is constant at 120 gal/min, the effluent temperatures are highest for the "best" performing battery and lowest for the poorest performing battery. The reverse is true once the voltage control system begins to reduce the flow rate, because the flow rate required to maintain the battery at 245 V is highest for the best performing battery.

rise faster than the predictions of the computer simulation. This apparent decrease in the Mk 67 battery's intrinsic voltage capabilities could be the result of H_2 recirculation.

Figures 27-29 present the agreement between the simulation and the observed results for the case of low temperature and low salinity. The predictions of the simulation are excellent between the 1½ and 7-min mark.

The discrepancies in the first 1½ min of the discharge are caused by starting transients. The battery is filled at a flow rate of 120 gal/min until the system pressure reaches 45 psig, whereupon the flow rate is reduced to the 30-40 gal/min required to bring the battery voltage up to the desired 245 V. The wide range of observed voltages found in the first 1½ min (Fig. 27) results from variations in the time it takes to accomplish this task. In contrast, the computer simulation simulates operation in which the filling time is very short with a flow control valve with infinitely fast and accurate response. This condition is best approached by the battery behavior given by the "leading edge" of the observed voltage envelope. It is significant that the agreement between the simulation and the leading edge is excellent.

Low temperature, low salinity discharges of the Mk 67 battery are frequently marked by clogging and electrical arcing within the battery in the period beyond 7½ min. This, along with the probable recirculation of H_2 , accounts for the poor performance during this period. Since the simulation assumes that no voltage losses from undesired effects such as arcing or clogging occur, a valid comparison during the latter portion of the discharge would be that of the trailing edge of the voltage envelope and the nominal predicted voltage line. These two lines are in good agreement, reaching the cutoff voltage of 160 V (0.7 V/cell) within 0.5 min of each other.

Thus, the nominal voltage predictions of the simulation are in excellent agreement for 95% of the discharge time to a cutoff voltage of 160 V if the leading edge of the voltage envelope is used during the first 1½ min of the discharge to compensate for the effects of start-up procedures and if the trailing edge of the voltage envelope is used beyond the 8-min mark to compensate for the effects of arcing and clogging.

The predicted temperatures (Fig. 28) and the flow rates (Fig. 29) are in good agreement with the observed results, especially when allowances are made for the starting transients and for the clogging and arcing which take place near the end of the discharges.

DISCUSSION

When limitations of the test facility and the effects of clogging and arcing are taken into account, the voltage, flow, and temperature predictions of the computer simulation are in good-to-excellent agreement with the observed

performance of the Mk 61 Mods 0 and 2, Mk 64, and Mk 67 batteries. The configurations of the four batteries used in this study are sufficiently diverse that these results are applicable to all high-drain, AgCl-Mg battery configurations known to this author. Furthermore, the temperature and salinity of the electrolytes used in the discharges reported here cover the extremes found in the world's oceans with the exception of a few small regions such as those at the bottom of the Red Sea where extremely warm concentrated brines are found. On this basis we conclude that the simulation is more than adequate for use in carrying out parametric studies or for the design of high-drain, sea water-activated batteries which use either AZ61 or AP65 magnesium alloy, the most common alloys for such batteries today.

APPLICATIONS

The computer cost of simulating a battery discharge ranges from \$15-\$30. The cost of discharging a full-size battery ranges from \$2,000 to \$30,000 (Ref. 1). In addition to the advantage of low cost, the simulation gives information on the spatial and temporal distributions of such quantities as temperature, electrolyte composition, and current density that are difficult or impossible to obtain from battery discharges. A further advantage of the simulation is that the range of operating conditions which can be studied is not limited by the availability of discharge facilities or by the practicality of tests conducted at sea. This latter is a significant problem, not only because of the high costs of field operations and instrumentation problems but because of the unpredictable occurrence of many of the test conditions which are of interest. Thus, the computer simulation permits rapid and inexpensive determinations of the behavior of competing battery configurations permitting a large reduction or even the complete elimination of the "cut and try" effort previously required to design batteries. The ability to evaluate the performance of candidate battery configurations for any desired operating condition considerably reduces the technological risks of battery development. These comments apply with equal force to system studies involving the application of high-drain, AgCl-Mg batteries.

ACKNOWLEDGMENT

Dr. William R. Davis, Assistant Director of the Applied Physics Laboratory, and staff, Mr. William Felton, Mr. Rodney Lipp, Mrs. Linda Rines and Mr. Robert Van Valkenburgh contributed to the success of this effort. Their contributions are gratefully acknowledged.

REFERENCES

1. APL-UW 7116, "A Computer Program for the Simulation of Water-Activated Silver Chloride-Magnesium Batteries; Its Basis and Operation," D. W. Faletti, Applied Physics Laboratory, University of Washington (in press)
2. D. W. Faletti and M. A. Gackstetter, "A Semi-Empirical Mathematical Model for Predicting the EMF of Small Silver Chloride-Magnesium Cells," J. Electrochem. Soc., 115, No. 12, 1210 (December 1968)
3. Personal communication, George Perkons, General Electric Co., Pittsfield, Mass.

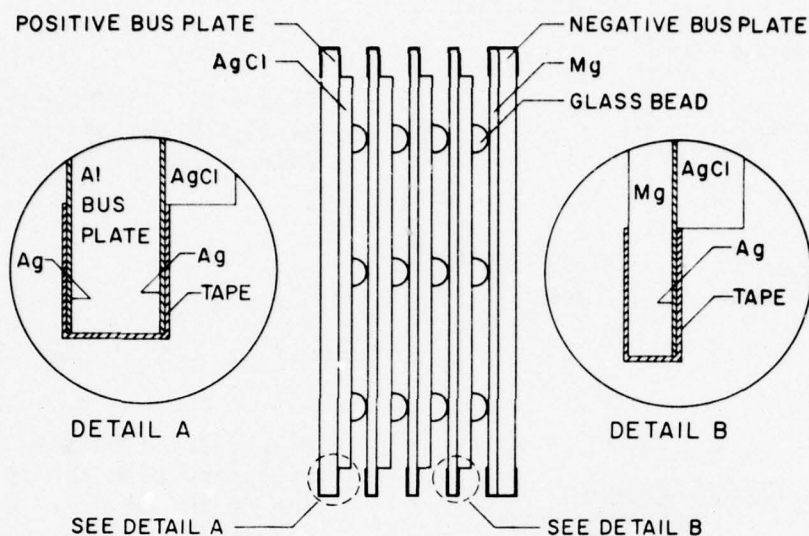


Figure 1. A four-cell series-connected section. The current is transferred to the load by bus rods (not shown). Glass beads imbedded in the AgCl provide interelectrode spaces through which the electrolyte passes. The silver foil provides electrical contact between the cells while acting as a barrier to chemical reactions between the AgCl and Mg. The edges of the magnesium-silver foil assemblies are taped to prevent electrolyte from reaching the back of the anodes.

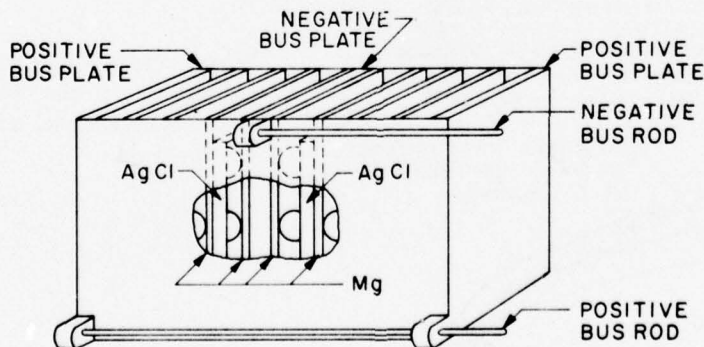


Figure 2. A battery composed of two series-connected sections, containing four cells each, which are connected in parallel. The cell assembly is of the same construction as that in Fig. 1, but there is symmetry about the negative bus plate.

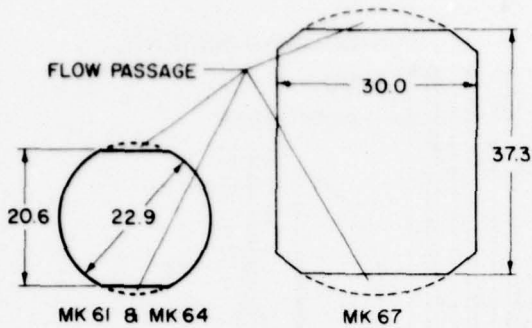


Figure 3. Configuration of the Mk 61, Mk 64, and Mk 67 cells. (dimensions in centimeters)

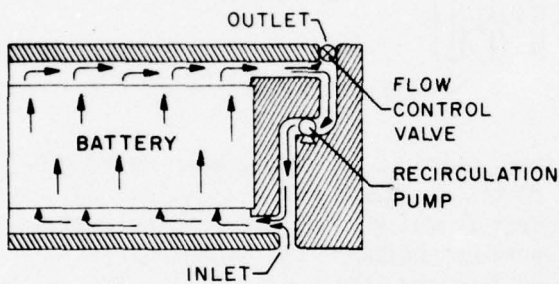


Figure 4. A battery compartment with provision for voltage control (as in the Mk 67). The entering electrolyte mixes with the portion of the battery effluent recycled by the recirculation pump before entering the flow passage under the battery. The intake flow of new electrolyte is adjusted by the flow control valve located at the exit.

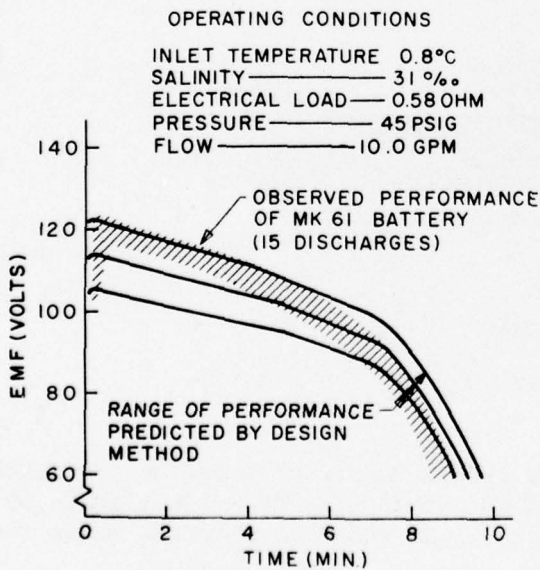


Figure 5. Predicted and observed voltages of the Mk 61 Mod 0 battery when discharged at low temperature.

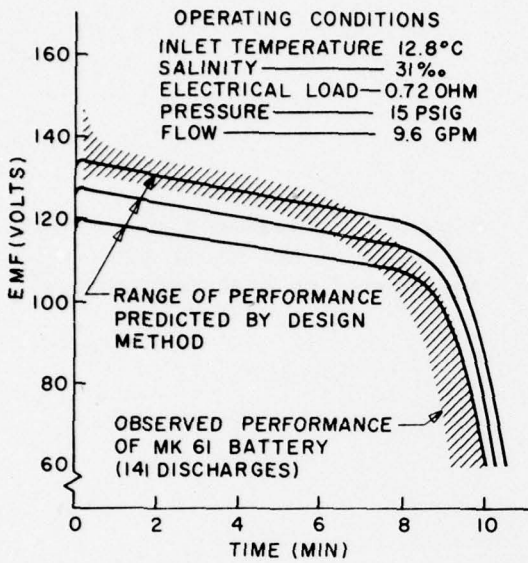


Figure 6. Predicted and observed voltages of the Mk 61 Mod 0 battery when discharged at 12.8°C.

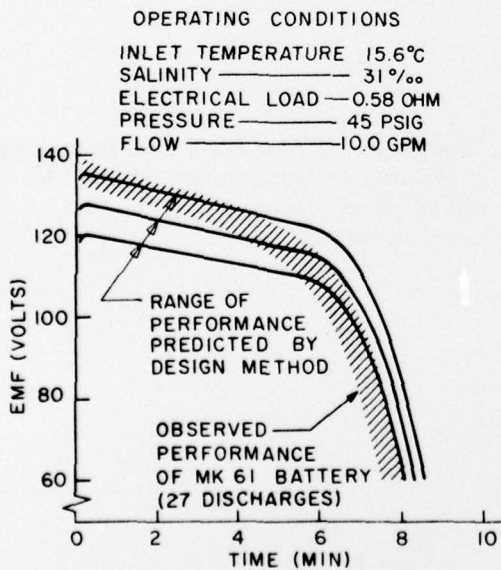


Figure 7. Predicted and observed voltages of the Mk 61 Mod 0 battery when discharged at 15.6°C.

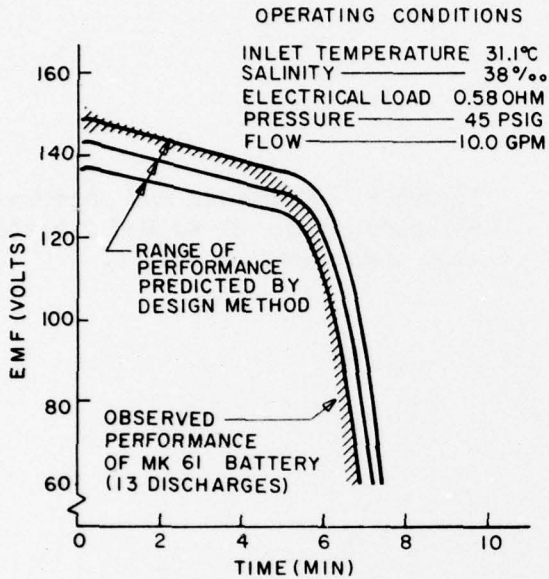


Figure 8. Predicted and observed voltages of the Mk 61 Mod 0 when discharged at high temperature.

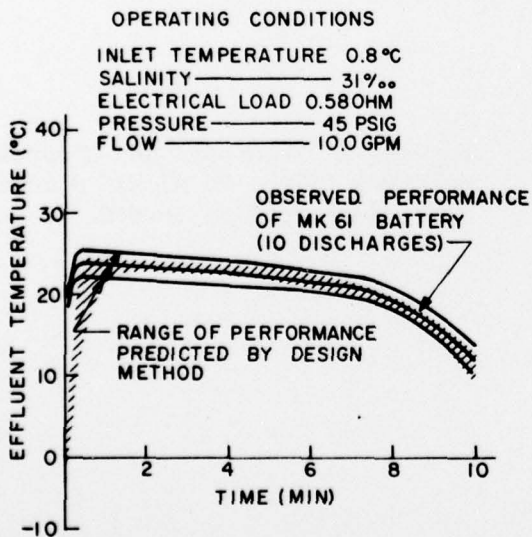


Figure 9. Predicted and observed effluent temperatures of the Mk 61 Mod 0 when discharged at low temperature.

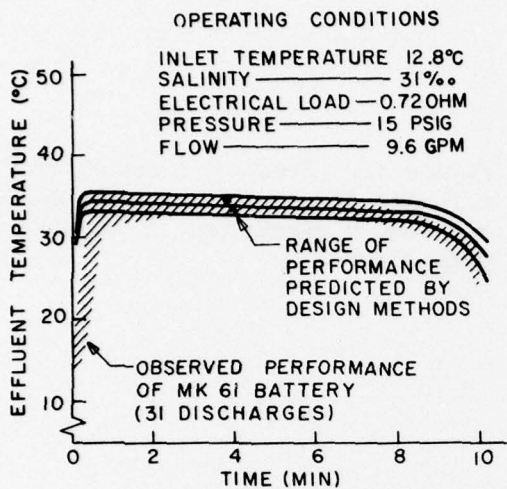


Figure 10. Predicted and observed effluent temperatures of the Mk 61 Mod 0 when discharged at 12.8°C.

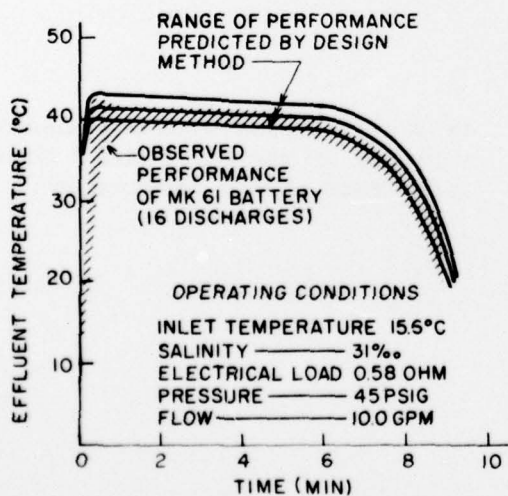


Figure 11. Predicted and observed effluent temperatures of the Mk 61 Mod 0 when discharged at 15.6°C.

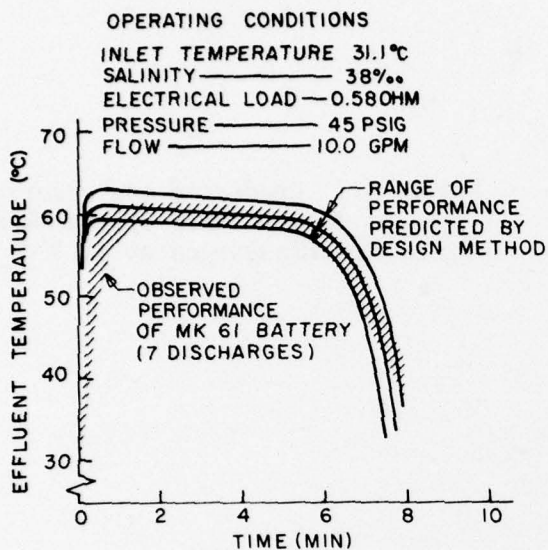


Figure 12. Predicted and observed effluent temperatures of the Mk 61 Mod 0 when discharged at high temperature.

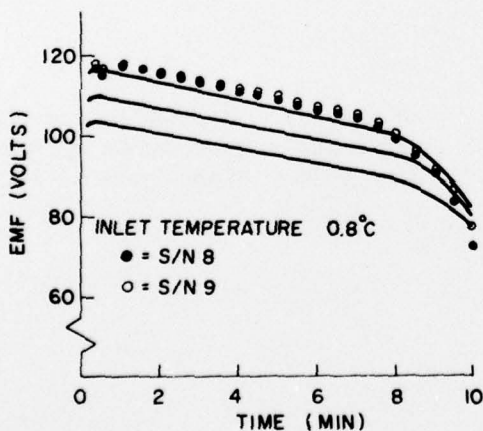


Figure 13. Predicted and observed voltages of the Mk 61 Mod 2 when discharged at low temperature.

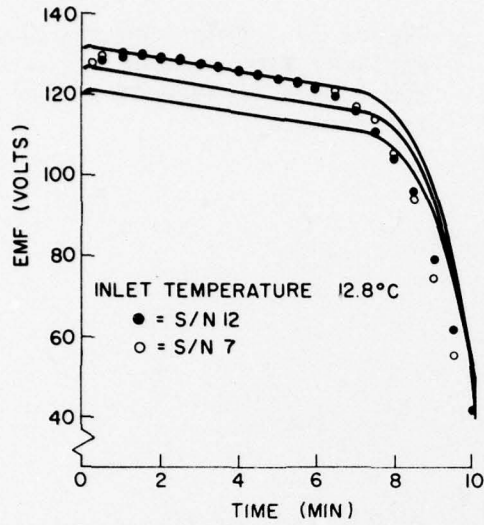


Figure 14. Predicted and observed voltages of the Mk 61 Mod 2 when discharged at 12.8°C.

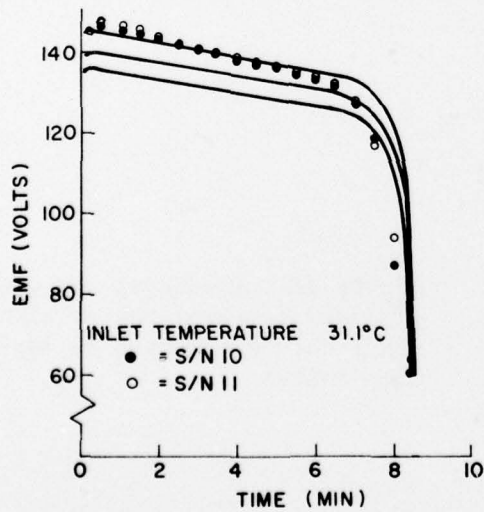


Figure 15. Predicted and observed voltages of the Mk 61 Mod 2 when discharged at high temperature.

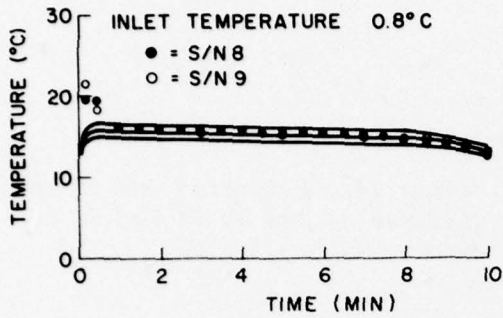


Figure 16. Predicted and observed effluent temperatures of the Mk 61 Mod 2 when discharged at low temperature.

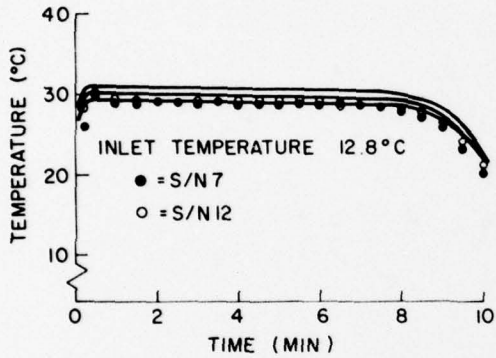


Figure 17. Predicted and observed effluent temperatures of the Mk 61 Mod 2 when discharged at 12.8°C.

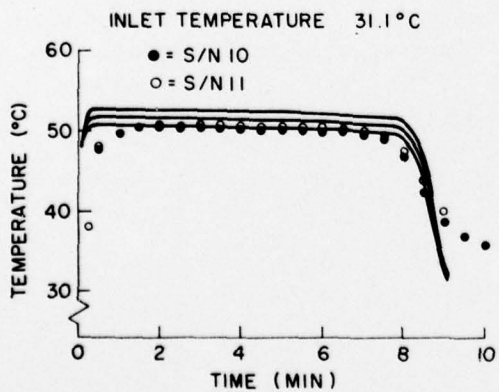


Figure 18. Predicted and observed effluent temperatures of the Mk 61 Mod 2 when discharged at high temperature.

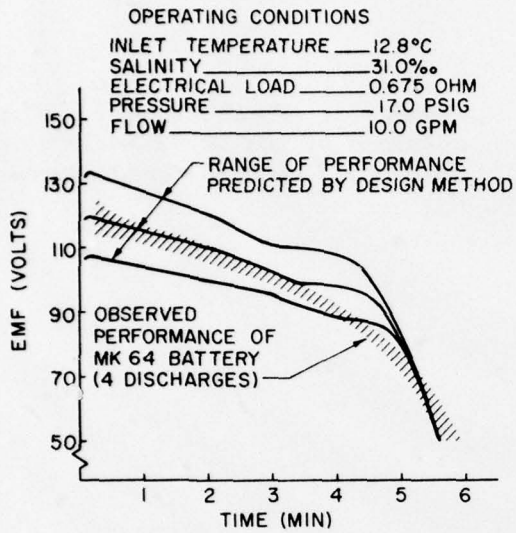


Figure 19. Predicted and observed voltages of the Mk 64 battery.

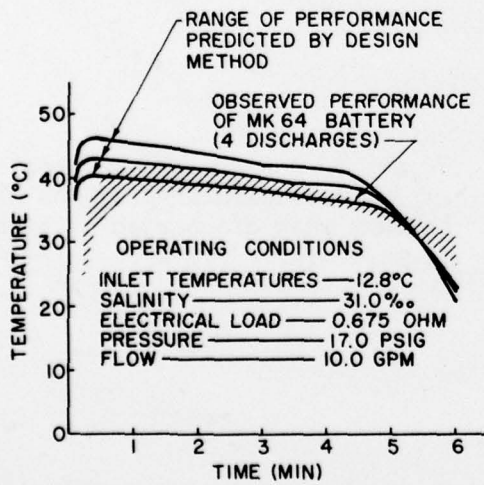


Figure 20. Predicted and observed effluent temperatures of the Mk 64 battery.

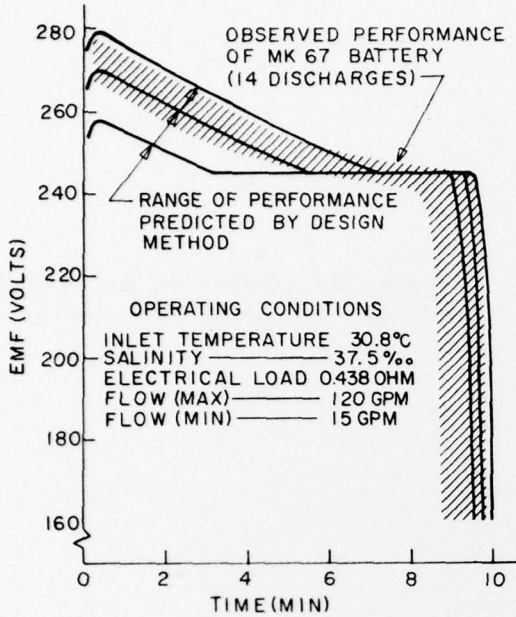


Figure 21. Predicted and observed voltages of the Mk 67 battery when discharged at high temperature.

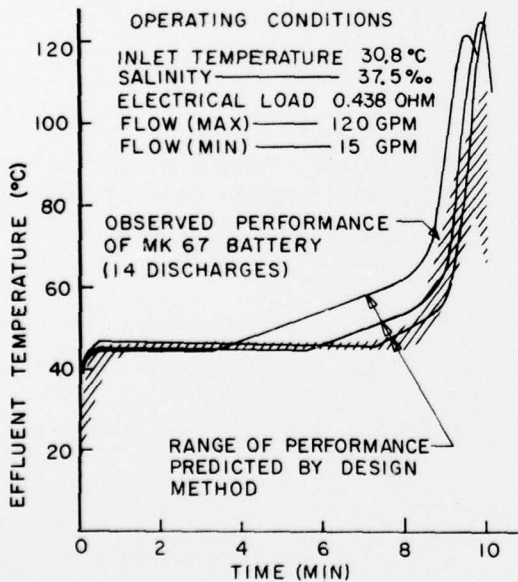


Figure 22. Predicted and observed effluent temperatures of the Mk 67 battery when discharged at high temperature.

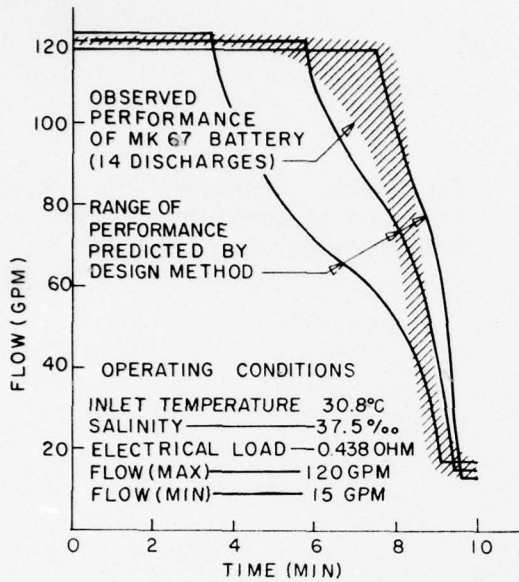


Figure 23. Predicted and observed flow rates of sea water entering the Mk 67 battery when discharged at high temperature.

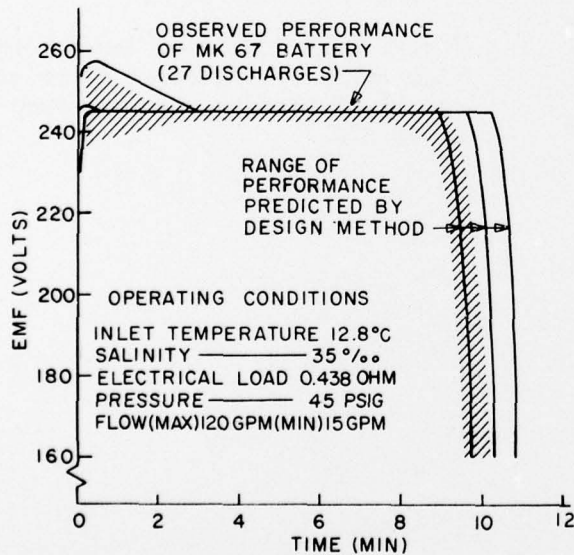


Figure 24. Predicted and observed voltages of the Mk 67 battery when discharged at 12.8°C.

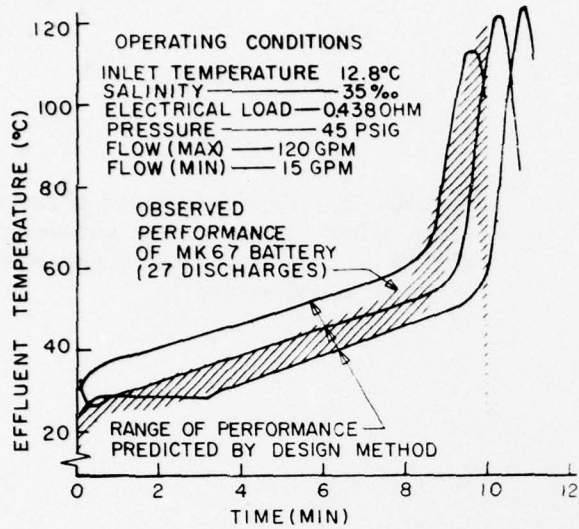


Figure 25. Predicted and observed effluent temperatures of the Mk 67 battery when discharged at 12.8°C.

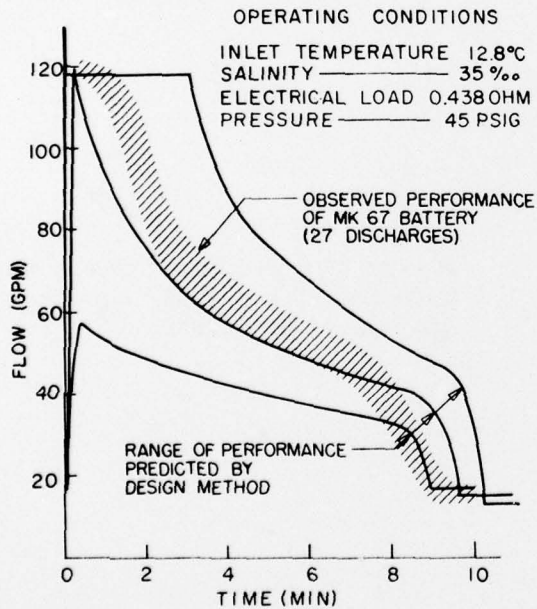


Figure 26. Predicted and observed flow rates of sea water entering the Mk 67 battery when discharged at 12.8°C.

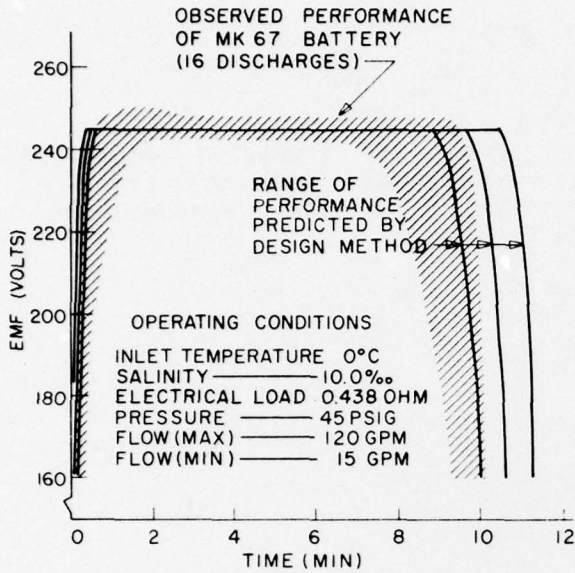


Figure 27. Predicted and observed voltages of the Mk 67 battery when discharged at 0°C.

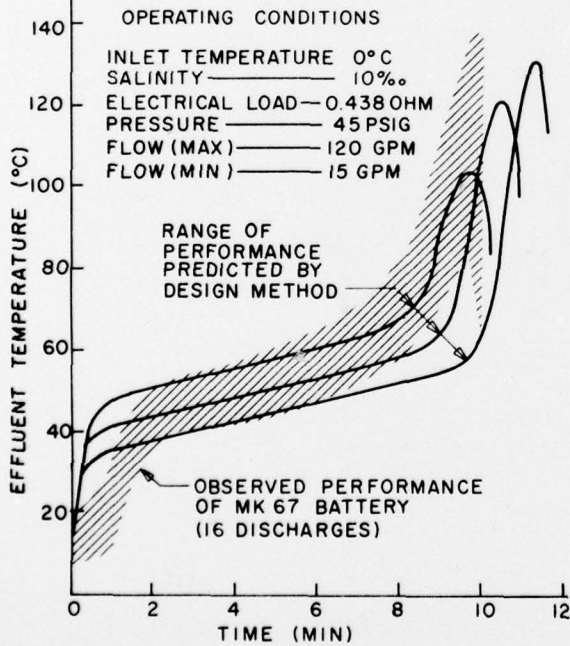
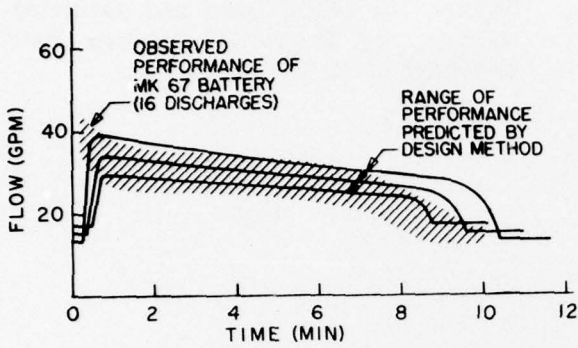


Figure 28. Predicted and observed effluent temperatures of the Mk 67 battery when discharged at 0°C.

OPERATING CONDITIONS

INLET TEMPERATURE — 0°C
 SALINITY — 10.0‰
 ELECTRICAL LOAD — 0.438 OHM
 PRESSURE — 45 PSIG

Figure 29. Predicted and observed flow rates of sea water entering the Mk 67 battery when discharged at 0°C.



UNCLASSIFIED

Security Classification

DOCUMENT CONTROL DATA - R&D

(Security classification of title, body of abstract and indexing annotation must be entered when the overall report is classified)

1 ORIGINATING ACTIVITY (Corporate author) Applied Physics Laboratory, University of Washington, 1013 NE 40th, Seattle, Wash. 98105		2a REPORT SECURITY CLASSIFICATION UNCLASSIFIED	
		2b GROUP	
3 REPORT TITLE COMPUTER SIMULATION OF FULL-SIZE, HIGH-DRAIN AgCl-Mg WATER- ACTIVATED BATTERIES WITH AZ61 AND AP65 ANODES (U)			
4 DESCRIPTIVE NOTES (Type of report and inclusive dates)			
5 AUTHOR(S) (Last name, first name, initial) Faletti, Duane W.			
6 REPORT DATE 15 September 1971		7a TOTAL NO. OF PAGES 26	7b NO. OF REFS 3
8a CONTRACT OR GRANT NO. N00017-71-C-1305		9a ORIGINATOR'S REPORT NUMBER(S) APL-UW 7112	
b PROJECT NO. Item 0001		9b OTHER REPORT NO(S) (Any other numbers that may be assigned this report)	
c			
d			
10 AVAILABILITY/LIMITATION NOTICES Distribution of this report is unlimited.			
DISTRIBUTION STATEMENT A Approved for public release; Distribution Unlimited			
11 SUPPLEMENTARY NOTES		12 SPONSORING MILITARY ACTIVITY Commander, Naval Ordnance Systems Command Department of the Navy Washington, D.C. 20360	
13 ABSTRACT The predictions of a computer simulation for high-drain, AgCl-Mg batteries are compared to the observed performance of four full-size AgCl-Mg batteries: the Mk 61 (Mod 0 and Mod 2), Mk 64 and Mk 67. The Mk 61 Mod 0, like the Mk 64 and Mk 67 batteries, uses AZ61 magnesium anodes; the Mk 61 Mod 2 uses the high voltage magnesium alloy, AP65. These four batteries differ sufficiently in their configurations and were discharged over a wide enough range of operating conditions to constitute a valid test of the com- puter simulation's capabilities. The simulation gave voltage predictions accurate to within 7% for over 90% of the discharge. Predictions for other useful parameters, such as electrolyte temperature, are also given. This simulation can eliminate the need for most of the cut and try effort presently required in AgCl-Mg battery development and should be helpful in system studies of this battery. (U)			

14. KEY WORDS	LINK A		LINK B		LINK C	
	ROLE	WT	ROLE	WT	ROLE	WT
AgCl-Mg batteries						
Water-activated batteries						
High-drain batteries						
AZ61 magnesium alloy						
AP65 magnesium alloy						
Computer simulations						
Simulations						
Modeling						
AgCl						
MG						

INSTRUCTIONS

1. ORIGINATING ACTIVITY: Enter the name and address of the contractor, subcontractor, grantee, Department of Defense activity or other organization (*corporate author*) issuing the report.

2a. REPORT SECURITY CLASSIFICATION: Enter the overall security classification of the report. Indicate whether "Restricted Data" is included. Marking is to be in accordance with appropriate security regulations.

2b. GROUP: Automatic downgrading is specified in DoD Directive 5200.10 and Armed Forces Industrial Manual. Enter the group number. Also, when applicable, show that optional markings have been used for Group 3 and Group 4 as authorized.

3. REPORT TITLE: Enter the complete report title in all capital letters. Titles in all cases should be unclassified. If a meaningful title cannot be selected without classification, show title classification in all capitals in parenthesis immediately following the title.

4. DESCRIPTIVE NOTES: If appropriate, enter the type of report, e.g., interim, progress, summary, annual, or final. Give the inclusive dates when a specific reporting period is covered.

5. AUTHOR(S): Enter the name(s) of author(s) as shown on or in the report. Enter last name, first name, middle initial. If military, show rank and branch of service. The name of the principal author is an absolute minimum requirement.

6. REPORT DATE: Enter the date of the report as day, month, year, or month, year. If more than one date appears on the report, use date of publication.

7a. TOTAL NUMBER OF PAGES: The total page count should follow normal pagination procedures, i.e., enter the number of pages containing information.

7b. NUMBER OF REFERENCES: Enter the total number of references cited in the report.

8a. CONTRACT OR GRANT NUMBER: If appropriate, enter the applicable number of the contract or grant under which the report was written.

8b, 8c, & 8d. PROJECT NUMBER: Enter the appropriate military department identification, such as project number, subproject number, system numbers, task number, etc.

9a. ORIGINATOR'S REPORT NUMBER(S): Enter the official report number by which the document will be identified and controlled by the originating activity. This number must be unique to this report.

9b. OTHER REPORT NUMBER(S): If the report has been assigned any other report numbers (*either by the originator or by the sponsor*), also enter this number(s).

10. AVAILABILITY/LIMITATION NOTICES: Enter any limitations on further dissemination of the report, other than those

imposed by security classification, using standard statements such as:

- (1) "Qualified requesters may obtain copies of this report from DDC."
- (2) "Foreign announcement and dissemination of this report by DDC is not authorized."
- (3) "U. S. Government agencies may obtain copies of this report directly from DDC. Other qualified DDC users shall request through _____."
- (4) "U. S. military agencies may obtain copies of this report directly from DDC. Other qualified users shall request through _____."
- (5) "All distribution of this report is controlled. Qualified DDC users shall request through _____."

If the report has been furnished to the Office of Technical Services, Department of Commerce, for sale to the public, indicate this fact and enter the price, if known.

11. SUPPLEMENTARY NOTES: Use for additional explanatory notes.

12. SPONSORING MILITARY ACTIVITY: Enter the name of the departmental project office or laboratory sponsoring (*paying for*) the research and development. Include address.

13. ABSTRACT: Enter an abstract giving a brief and factual summary of the document indicative of the report, even though it may also appear elsewhere in the body of the technical report. If additional space is required, a continuation sheet shall be attached.

It is highly desirable that the abstract of classified reports be unclassified. Each paragraph of the abstract shall end with an indication of the military security classification of the information in the paragraph, represented as (TS), (S), (C), or (U).

There is no limitation on the length of the abstract. However, the suggested length is from 150 to 225 words.

14. KEY WORDS: Key words are technically meaningful terms or short phrases that characterize a report and may be used as index entries for cataloging the report. Key words must be selected so that no security classification is required. Identifiers, such as equipment model designation, trade name, military project code name, geographic location, may be used as key words but will be followed by an indication of technical context. The assignment of links, roles, and weights is optional.